



## **MECHANICAL PROPERTIES OF LIME-BASED MASONRY BLOCKS IN EUROPE\***

**Gero A. Marzahn<sup>1</sup>**

### **Abstract**

This paper investigates mechanical properties, such as strength and deformation parameters, under short-term and long-term loading conditions on lime-based masonry blocks. Beyond basic properties, which are required by testing standards for masonry products, the paper's focus is on mechanical characteristics whose testing is not required by current standards. Deformation-controlled tests were used to observe stress-strain relationships of blocks in pre- and post-peak range as well as values of compressive and tensile axial strength. Deformation parameters, such as Young's modulus and Poisson's ratio, could also be inferred from the tests. Masonry block trials with long-lasting compression loads were used to determine sustainable strength, and to obtain insights into the creep and shrinkage behavior of the block materials.

### **Keywords**

Blocks, compression, tension, stress, strain, lime, calcium silicate, autoclaved aerated concrete

---

\* © Copyright NLA Building Lime Group 2005

The views presented in this paper are solely those of the authors. The National Lime Association (NLA) and the Building Lime Group assume no liability or responsibility for any errors, omissions, or other limitations in this paper or for any products, services, or methods presented. This paper is intended for use by professional personnel competent to evaluate the significance and limitations of the information provided and who will accept full responsibility for the application of this information. NLA and the Building Lime Group do not intend to infringe on any patent or other intellectual property right or induce any other party to do so, and thus users of this document are responsible for determining whether any method, technique, or technology described herein is protected by patent or other legal restriction.

<sup>1</sup> Gero A. Marzahn, Dr.-Ing., University of Leipzig, Institute for Concrete Structures and Structural Materials, Leipzig, 04109, Germany and Northrhine-Westfalia Dept. of Transportation, 50679 Cologne, Germany, G.Marzahn@gmx.de

# 1 Introduction

The load-carrying capacity of masonry is primarily determined by properties of its components: masonry blocks and mortar. Blocks of calcium silicates or aerated concrete blocks using lime as a binding agent are popular in Europe and will be in the focus of discussion. By means of simplified and standardized material investigations, mainly compression tests of blocks and mortar trials, basic material characteristics were obtained to predict the failure load in a practical and generally sufficient manner. However, those basic fundamentals are not adequate to describe particular conditions for further differentiation in structural behavior or more comprehensive investigations, e.g., micro modeling of computational elements for masonry simulation or analysis of failure conditions. Therefore, additional material parameters, whose determination often go beyond those of existing masonry standards, are needed to describe a distinct behavior more accurately. Although masonry scholarship has a long and outstanding tradition, knowledge about masonry block behavior under different loading conditions, for example, is not well developed in comparison to that of other structural materials such as concrete. Consequently, several test series were performed in this study to focus on the determination of mechanical properties of two types of masonry blocks: calcium silicate blocks (CS1, CS2) and autoclaved aerated concrete blocks (AAC1, AAC2). Different strength and density classifications were considered. The test procedures used were aligned with German or European masonry standards, or followed the schemes of concrete tests, as needed.

## 2 Depth and density

In this study, different types of masonry blocks [calcium silicates (CS) and autoclaved aerated concrete blocks (AAC)] with different strengths were subjected to a variety of compression and tension loadings. The shape and density properties were determined according to German and European standards DIN 106, DIN 4165, and DIN EN 772 and are shown in Table 1. All blocks met the strength and density requirements of their respective standards.

Table 1 Shape and density properties of masonry blocks (1 inch = 25.4 mm, 1 lb/ft<sup>3</sup> = 0.016 kg/dm<sup>3</sup>)

Quantity		Calcium silicate		Autoclaved aerated concrete	
		CS1	CS2	AAC1	AAC2
Depths L/W/H	mm	500 / 240 / 238		500 / 240 / 200	
Density, gross	kg/dm <sup>3</sup>	1.857	1.864	0.544	0.450

## 3 Compressive strength

Several kinds of compressive strength tests were performed: compressive strength of standardized block according to German and European standards (DIN 106, DIN 4165, DIN EN 772); compressive strength of blocks longitudinally; and compressive strength of cylinders drilled out of solid blocks.

### 3.1 Standardized compressive strength

Standardized compressive strength tests were performed on masonry blocks as the basis for their strength classification. Shape factors, which take into account the dependency of the test results on the shape of the specimen, were considered in calculating the strength values that are summarized in Table 2.

### 3.2 Longitudinal Compressive Strength

Masonry structures subjected to bending moments may experience compression acting longitudinal to the blocks; therefore, this kind of load resistance is important to consider as well. Although no test procedure currently exists to measure longitudinal compressive strength, blocks placed in an upright

position were subjected to compression in the same manner as would be applied in standardized compression tests. Due to their greater slenderness, the longitudinal blocks had a lower compressive strength than the block compressive strength adjusted to test standards (Table 2). In addition, no shape factors had to be taken into account because of the lack of comparability.

### 3.3 Uniaxial Compressive Strength

The compressive strength of cylinders is widely accepted in concrete technology. Cylinders offer the advantage of a variety of slenderness ratios of specimens. Drilled from solid blocks, the cylinders used in these tests had a diameter of  $d = 100$  mm and a height of  $h = 200$  mm, leading to a slenderness ratio of  $h/d = 2$ , approximately twice that of masonry blocks used in standardized block test schemes. The load was strain-control-applied, so that both the ascending and the descending parts of the stress-strain diagram were monitored. By means of energetic considerations and characteristic values of the stress-strain curve, the material's behavior under service and ultimate load conditions, as well as the collapse conditions, were inferred. Independent of the material, failure occurred as a shear failure in a plane inclined by 45 to 60 degrees horizontally (Figure 1c). Whereas the broken material appeared smooth to slightly roughed-up in the autoclaved aerated concrete, the cracks did not extend through the aggregates in the calcium silicate blocks and created a characteristic aggregate interlocking. The measured cylinder compressive strength, that might be interpreted as uniaxial compressive strength (Kirtschig 1981, Schickert 1980, Schlee 1975), reached magnitudes of only 60 (calcium silicates) to 90 percent (autoclaved aerated concrete) of that of the standardized compression test on the units (Table 2).

Table 2 Compressive strength of masonry blocks (1 psi = 0.0069 N/mm<sup>2</sup>)

Block	Standardized compressive strength $f_b$ N/mm <sup>2</sup>	Longitudinal compressive strength $f_{b,l}$ N/mm <sup>2</sup>	Uniaxial compressive strength $f_{b,cyl}$ N/mm <sup>2</sup>	Young's modulus $E_b$ N/mm <sup>2</sup>
CS1	25.90	—1)	17.10	10,088
CS2	20.91	10.27	12.78	9,908
AAC1	4.11	3.17	3.85	1,938
AAC2	3.21	1.77	2.79	1,516

1) not obtained

## 4 Deformation Capacity under Compression

### 4.1 Stress-Strain Relationship

A loaded masonry block generates deformations that influence the bearing capacity, which in turn influences the generation of deformations. The relationship between loading and deformation can be illustrated using stress-strain relationships. Although masonry specimens were primarily stress-control loaded in the past, the present test equipment enabled the use of deformation-controlled tests as well, which are better suited for a more comprehensive investigation and are state-of-the-art in concrete technology. Constant strain increments, rather than stress increments, enabled a steady loading and test run in peak as well as in the post-peak range, so that facts about degradation, strain softening, failure mechanism, and the final progressive collapse became visible.

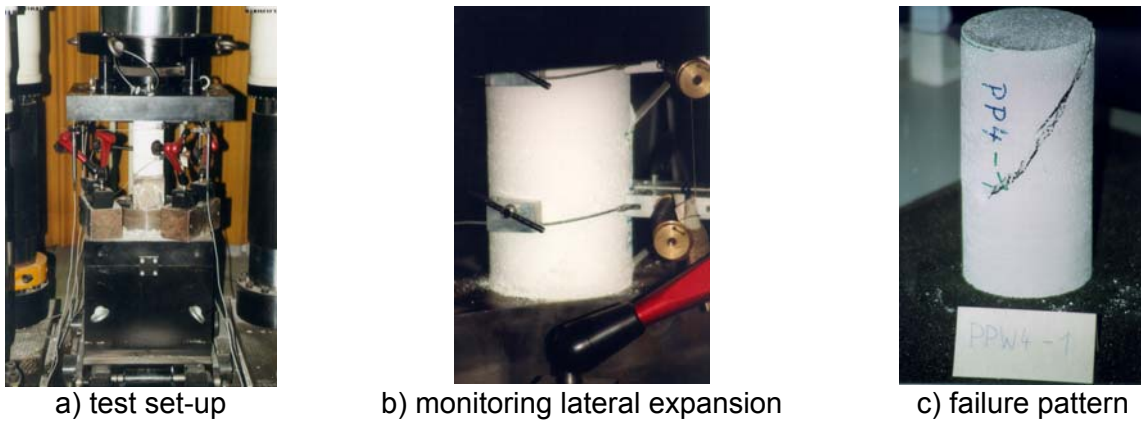


Figure 1 Deformation-controlled compression test of AAC cylinders

This test set-up was adopted for cylindrical test specimens. The controlling parameters were both the longitudinal and the transverse deformation of the cylinder, measured by means of three vertical linear variable differential transformers (LVDTs) spaced around the cylinder and two horizontal LVDTs at one-third and two-thirds of the cylinder height, respectively (Figure 1a, b). The loading rate was approximately 5/10,000 mm per second and was governed primarily by the vertical strain increase, but was even lower at 1/10,000 mm per second when transverse strains grew non-proportionally. The ratio between stresses and strains are illustrated in the stress-strain diagrams in Figure 2.

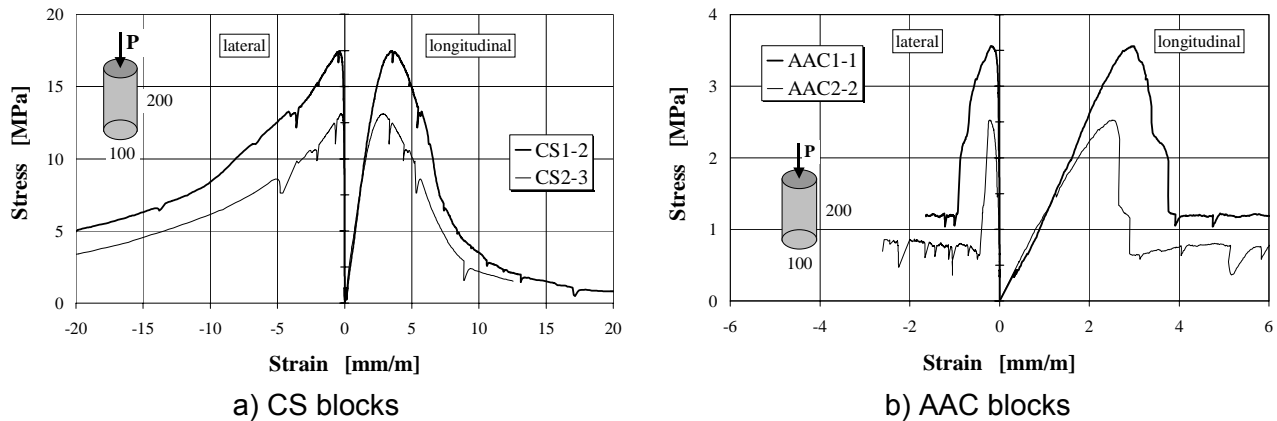


Figure 2 Stress-strain relationship for masonry blocks

As the compressive strength of materials increased, the ascending stress-strain path became more vertical, resulting in a reduction of curvature. This is a sign that with growing strength, not only did the elastic properties become stiffer, but also the failure altered to become more brittle and less ductile. The higher the strength for each of the tested materials, the more abruptly the collapse occurred and the more steeply the descending stress-strain line in the post-peak area fell. The testing established that the calcium silicates (CS) definitely behaved more ductilely than the autoclaved aerated concrete blocks (AAC).

The longitudinal strains measured under maximum stresses are illustrated in Figure 3. With enhanced compressive strength, those strains also reached greater values. The intensity of increase was significantly higher for AACs. This is primarily due to the more homogenous texture of the AAC material, which forces the blocks to react more elastically rather than plastically by delaying micro-cracking. Unexpectedly, the CS blocks fully developed their strength at a strain of approximately 3 mm per m, which is beyond the fixed 2 mm per m of the characteristic stress-strain relationship given

in the European masonry standard Eurocode 6 (ENV 1996). The code value might overestimate the computed material resistance to compression or bending. Further research is required in this area.

## 4.2 Young's Modulus

The elastic material behavior characterized by linear proportionality between stresses and strains is described by the elastic, or Young's, modulus. This can be determined separately by means of specific tests (DIN 1048), or it can be concluded from the plotted stress-strain diagram. As widely applied to masonry structures, the Young's modulus is the slope of a secant between the origin and, usually, the point that equals one-third of the maximum stress after first loading, which is known as  $E_{33}$  (Figure 4).

The Young's modulus is linearly dependent on the cylinder's compressive strength and may be calculated from equation [1] (Marzahn 2000):

$$E_{33} = 450 \cdot f_{b,cyl} \quad (1)$$

Values to be combined should be measured on the same-shaped specimens, e.g., the elastic modulus and the strength values should be developed on cylinders alone and not mixed with results obtained from testing of cubes.

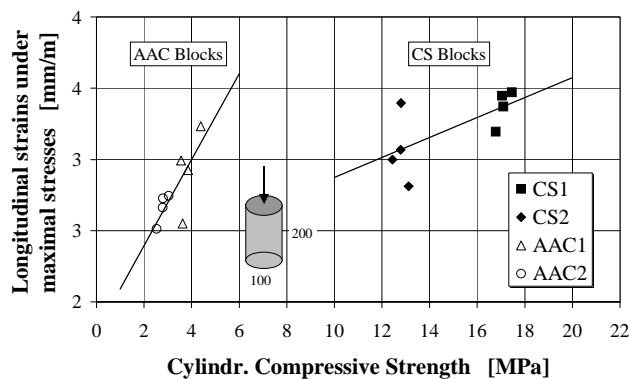


Figure 3 Longitudinal strains under maximal stresses

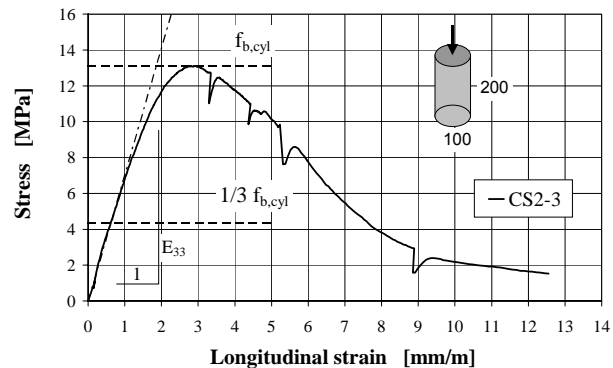


Figure 4 Determination of the elastic modulus  $E_{33}$  (Young's modulus)

## 4.3 Poisson's Ratio

The uniaxial compression test also provided the opportunity to measure both the longitudinal and the lateral deformation of the cylinders. From this, the Poisson's ratio at one-third of the maximum stress level,  $\varepsilon_{33}$ , and the lateral modulus of elasticity,  $E_{33,q}$ , were calculated. Under small loads, both the lateral and the longitudinal strains developed proportionally, so that the Poisson's ratio remained constant. Above the service load level (40 percent of the maximum load level for AAC and 70 percent of the maximum load for the calcium silicate), the blocks showed an elastic degradation due to an increased lateral expansion. The intensity of augmentation of the CS blocks surpassed that of the AAC blocks. For calculation purposes under service loads, a constant Poisson's ratio of about 0.10 for CS blocks and 0.20 for AAC blocks can be assumed. The magnitude of the elastic modulus in the lateral direction was dispersed, but it can be limited to between five and ten times the elastic modulus in the longitudinal direction.

## 5 Tensile Strength

Tensile strength describes the capacity of a material when subjected to maximum tension. Depending on the mode of loading, the tensile strength is differentiated into flexural tensile strength, splitting tensile strength, and axial or direct tensile strength. Standardized test procedures for testing the tensile strength of masonry units currently do not exist in Germany; therefore, the tensile strength test set-up was adopted from the concrete testing model.

### 5.1 Flexural Tensile Strength

The flexural tensile strength was measured on solid blocks subjected to a stress-controlled load applied to the center between the two supports at the ends of the blocks (Figure 5). The loading rate was approximately 0.10 N/mm<sup>2</sup> per second for AAC blocks and 0.50 N/mm<sup>2</sup> for CS blocks. The span of 4/5 of the block length did not allow a pure bending because of shear distortion in the cross sections. By means of 3D finite element calculation, a correction parameter ( $k = 0.922$ ) was inferred by which the measured ultimate bending stresses were multiplied, thus yielding approximated pure flexural tensile strength values. The average tensile strengths are outlined in Table 3.

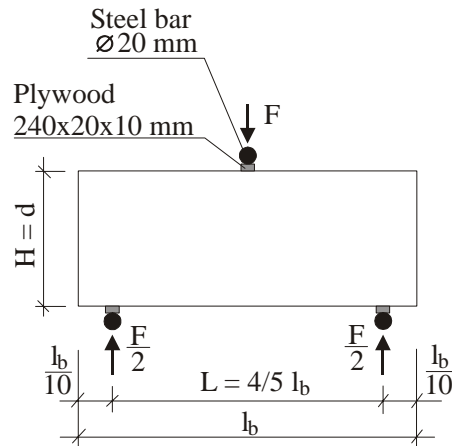


Figure 5 Determining the flexural strength

Table 3 Tensile strength values of solid blocks, mean values (1 psi = 0.0069 N/mm<sup>2</sup>)

Block	Flexural tensile strength $f_{b,f}$ N/mm <sup>2</sup>	Splitting tensile strength $f_{b,sp}$ N/mm <sup>2</sup>	Axial tensile strength $f_{b,ax}$ N/mm <sup>2</sup>
CS1	2.21	1.19	1.421)
CS2	1.99	0.95	1.56
AAC1	0.93	0.33	0.95
AAC2	0.57	0.27	0.46

1) only one value

### 5.2 Splitting Tensile Strength

Due to the convenience of determining splitting strength as well as its reduced sensitivity to moisture influences, splitting strength is commonly substituted for all kinds of tensile strengths of masonry units. According to Schubert, it makes no difference whether solid blocks are split in a longitudinal or cross-sectional direction (Schubert/Gonzales 1997, Schubert/Friede 1980). For this test set-up, all

blocks were split longitudinally, parallel to the block length (Figure 6). The load was applied incrementally to the splitting area at a loading rate of 0.05 N/mm<sup>2</sup> per second. The failure occurred between 20 and 30 seconds after loading for each of the samples.

### 5.3 Axial Tensile Strength

Direct or axial tensile strength is a very important material parameter because it represents a pure material strength quantity, which also has tremendous influence on the derivation of multi-axial strength characteristics. Generally, complicated test procedures lead to difficult and more expensive test runs; hence, such tests are usually avoided. However, in this case, direct tension tests were carried out on cylindrical specimens with 100 mm height and 100 mm diameter. Steel plates glued with epoxy resin on the top and bottom faces of the cylinders were used to apply the tensile force. Soon after the plates were glued, the specimens were tested to reduce additional shear stresses in the interfaces of the steel-masonry block, which might have been generated by restrained shrinkage of the adhesive, differences in elastic modulus between the steel and masonry units, or inequality of Poisson's ratio of the different materials. Figure 7 illustrates the test set-up after the test was performed. Most often, the failure occurred in the middle of the cylinder height rather than at the glued interfaces. The test results are recorded in Table 3. Almost all axial strength values are below those of corresponding splitting or bending test values and show a greater spread.

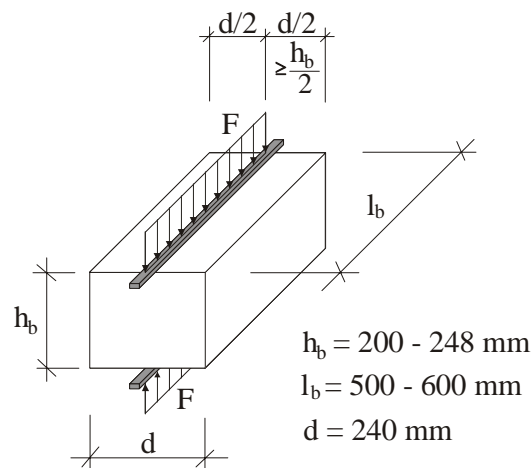


Figure 6 Determining the splitting strength

Although a linear relationship between tensile and compressive strength may be assumed for each kind of block material as a first estimation, this is not applicable as a general rule. As a matter of fact, the tensile strength grows at a lower rate and non-proportionally to compressive strength. In addition, comparisons are useful only when results are obtained on the same kind of specimens, e.g., to compare results from cylindrical specimens only or cubes only. Hence, the ratio between direct tensile strength and uniaxial compressive strength of cylinders drilled from solid blocks is plotted in Figure 8.



Figure 7 Direct tension test after test run

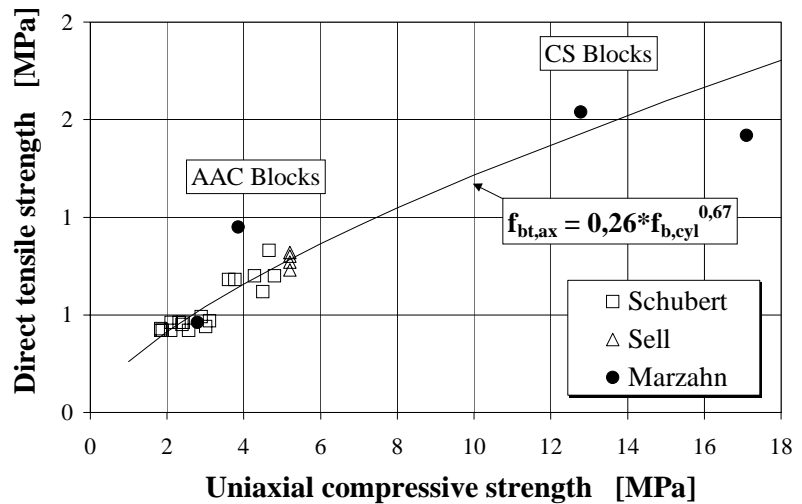


Figure 8 Relationship between direct tensile strength and uniaxial compressive strength of masonry block cylinders (reference values by Schubert/Gonzales (1997) and Sell (1970))

Obviously, there is a potential relationship between the direct tensile strength and uniaxial compressive strength, similar to that of concrete (Hilsdorf 1997), where the compressive strength,  $f_{b,cyl}$ , to the power of two-thirds yields the direct tensile strength,  $f_{bt,ax}$ :

$$f_{bt,ax} = 0.26 \cdot f_{b,cyl}^{0.67} \quad (2)$$

The different kinds of tensile strengths may be substituted for each other, but not on a one-to-one basis, as was often assumed in the past. Rather, the axial tensile strength,  $f_{bt,ax}$ , is about 72 percent of the splitting tensile strength,  $f_{bt,sp}$ :

$$f_{bt,ax} = 0.72 \cdot f_{bt,sp} \quad (3)$$

and only 50 percent of the flexural tensile strength,  $f_{bt,fl}$  (Marzahn 2000):

$$f_{bt,ax} = 0.50 \cdot f_{bt,fl} \quad (4)$$

Both the Eurocode 2 (ENV 1992) and the Model Code 90 (CEB-FIP Model Code 1990) emphasize a linear relationship between different kinds of tensile strengths, but the correlation factors inferred for concrete seem to overestimate the ratios for masonry materials other than concrete.

## 6 Long-Term Behavior

Aside from deformation under short-term loading, masonry blocks also experience time-dependent deformations, which may or may not be caused by loads. Whereas shrinkage is independent of loading, creep is generated by long-lasting loads. Both creep and shrinkage were of interest in this study. Additionally, when blocks are subjected to high compression loads, they may fail at a load level below the instantaneous compressive strength. For this reason, an additional test series was conducted that focused on determination of the sustainable compressive strength.

## 6.1 Creep and Shrinkage

In this study, specimens from calcium silicates (CS1, CS2) and autoclaved aerated concrete blocks (AAC1, AAC2) with different strengths were subjected to compression loading at a variety of levels. The specimens were formed using three courses of half blocks laid dry on top of each other (Figure 9). For each specimen set, two specimens were built, permitting eight tests in total. Before using the blocks for testing, all specimens were stored for six weeks under constant climate conditions (22°C, 55 percent relative air humidity) to allow the blocks to attain moisture equilibrium with the ambient air. The moisture contents measured at the beginning of the creep tests were 1 to 3 percent of weight for CS blocks and 2 to 5 percent of weight for AAC blocks. The deformation was monitored by LVDTs over one block. A loading frame provided the sustained dead load of 24 kN (0.5 MPa) and 48 kN (1.0 MPa), respectively, corresponding to ratios of 0.05 and 0.10 (CS) as well as 0.15 and 0.35 (AAC) of the observed instantaneous uniaxial compressive strength. Because of the low stress levels, a linear relationship between stresses and creep strains was expected. Compensation for shrinkage was made on unstressed specimens in the same environment and from the same material, equal in shape and size to the loaded specimens. Both the shrinkage strains of those control specimens,  $\varepsilon_{bs,t}$ , and the spontaneous strains after loading,  $\varepsilon_{b,t0}$ , were subtracted from the total strains,  $\varepsilon_{b,t}$ , of the stressed specimens to determine creep strains,  $\varepsilon_{bc,t}$ :

$$\varepsilon_{bc,t} = \varepsilon_{b,t} - \varepsilon_{b,t0} - \varepsilon_{bs,t} \quad (5)$$

The creep strain grew with decreasing intensity as time went on, manifesting the biggest gains within the first days after loading (Figure 10). Although bearing the same load level, the AAC blocks showed a four-times greater creep than the CS blocks, and the AAC2 units demonstrated creep up to twice that of the AAC1 units. This indicates that both the material and the strength of the material have a strong influence on creep.

Because of the proportionality between sustained stresses and strains, creep strains may be expressed in relation to elastic strains. The proportionality factor between the two is called the creep coefficient,  $\phi_{b,t}$ , and may be expressed as:

$$\varepsilon_{bc,t} = \phi_{b,t} \cdot \frac{\sigma}{E_b} \quad (6)$$

where  $\varepsilon_{bc,t}$  is the creep strain,  $\sigma$  are the sustained stresses,  $E_b$  is the elastic modulus of the blocks, and  $\phi_{b,t}$  is the creep coefficient. Despite the fact that the creep coefficient is not a constant and is, in fact, time dependent, the maximum creep is primarily of interest for design purposes. Hence, the ultimate creep coefficient,  $\phi_{b,\infty}$ , in infinite time can be obtained by using the hyperbola function of Ross (Ross 1937). The ultimate shrinkage values have been similarly developed. The final values for creep and shrinkage and the inferred ultimate creep coefficient are summarized in Table 4. The shrinkage is only differentiated between the two materials, CS and AAC.

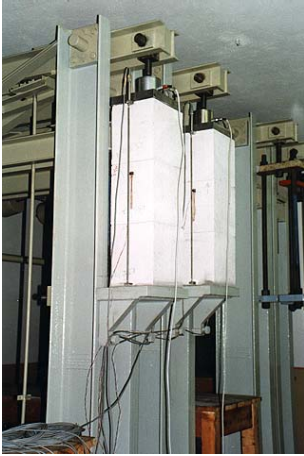


Figure 9 Loading arrangement

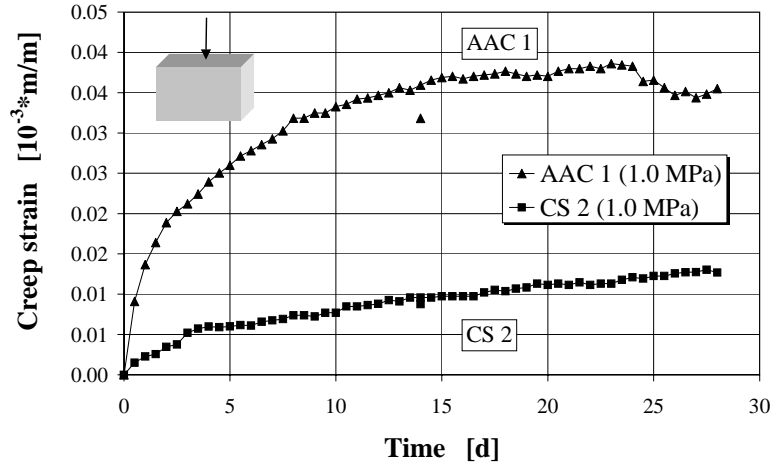


Figure 10 Creep strains of CS2 and AAC1 blocks subjected to compressive stresses of 1.0 MPa

The development of the creep coefficient for AAC units (AAC1, AAC2) is illustrated in Figure 11. First, the growth rate of  $\phi_{b,t}$  for both AAC1 and AAC2 blocks decreases with time and ultimately approaches a final value. Second,  $\phi_{b,t}$  is not affected by stresses because the magnitude of the creep coefficient is the same for both units despite different load levels.

Table 4 Final creep and shrinkage parameters of masonry blocks

Block	Final creep strains $\epsilon_{bcr,\infty}$ mm/m	Ultimate creep coefficient $\phi_{b,\infty}$ —	Final shrinkage strains $\epsilon_{bs,\infty}$ mm/m
CS1	~0.02	~1.00	0.050 – 0.070
CS2	0.02	0.60	
AAC1	0.03	0.15	0.030 – 0.040
AAC2	0.10	0.25	

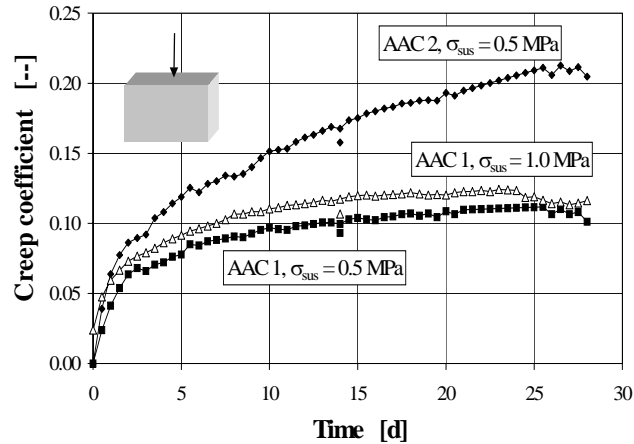


Figure 11 Creep coefficients for AAC blocks

## 6.2 Sustainable Strength

This test series focused on sustainable compressive strength. Small cylinders (diameter 50 mm, height 100 mm) were drilled out of each kind of solid block (CS1, CS2, AAC1, AAC2) for use as specimens. Knowledge about the sustainable strength of masonry blocks is very limited and for practical reasons, primarily borrowed from concrete. For concrete, the ratio between long-term and short-term compressive strength is around 0.85 (Hilsdorf 1997). Furthermore, if a concrete specimen is excessively loaded, the specimen will fail within the first seven days; otherwise, it will never fail under this load level (Hilsdorf 1997). The tests, therefore, were designed to put stresses up to 80 and 90 percent of the uniaxial compressive strength,  $f_{bt,fl}$ , on each cylinder for a period of seven days.

Whereas the specimens loaded with  $0.8 \cdot f_{b,cyl}$  did not fail, most of the specimens (CS1, AAC2) collapsed within the first two hours of load impact when the load level reached  $0.9 \cdot f_{b,cyl}$ . The reason why two of the massive cylinders did not fail may be a function of the spread of the strength values (Figure 12).

A conclusion can be inferred that the ratio between sustainable and instantaneous compressive strength for both calcium silicate and autoclaved aerated concrete blocks is approximately 0.80 up to 0.85. The ratio itself is not influenced by the material nor by the material strength. This result is consistent with the knowledge of other mineral construction materials.

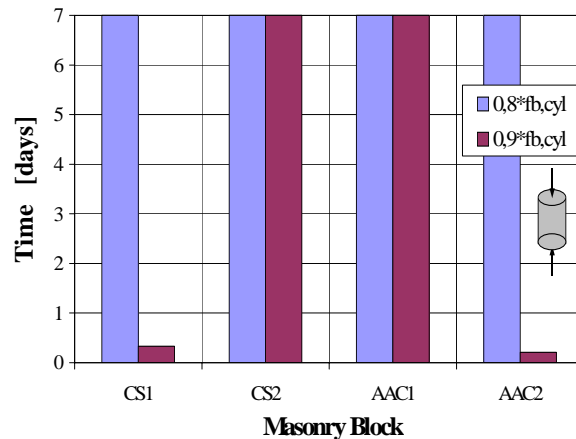


Figure 12 Time that specimens withstood the permanent compression load

## 7 Conclusions

Different kinds of compressive and tensile strength of solid masonry blocks were determined and compared. Moreover, by means of deformation-controlled compression tests, it was also possible to monitor the ascending as well as the descending part of the stress-strain relationship pointing to the failure behavior – brittle or ductile – and to characteristic stress-strain pairs. By knowing the exact failure mechanism, correct predictions for redistribution of internal loads and the progressive collapse behavior were possible. The comparison of uniaxial tensile and compressive strength resulted in a correlation that is known from concrete patterns, where the compressive strength to the power of two-thirds may express the direct tensile strength. The sustainable strength tests led to insights into the long-term deformation behavior of solid masonry blocks. Relationships and influences similar to those of concrete were found. As long as moderate stresses are permanently applied, the creep develops proportionally with stresses over time. The kind of material and the material strength as well as climate and loading conditions have a primary impact on creep.

The aforementioned test results describe material properties that influence the bearing capacity of masonry blocks and, consequently, masonry structures as well. Determination of these material properties is often beyond the current material testing standards. Especially when materials are heavily loaded, or when design rules need to be validated and made more accurate, correct material properties are essential. It is desirable and advantageous, therefore, to study deficiencies of mechanical properties of blocks, mortar, and masonry in order to introduce new skills and experiences into the daily design process.

## References

- CEB-FIP Model Code 1990, Design Code, Thomas Telford, London, United Kingdom, 1998
- DIN 106, Kalksandsteine – Vollsteine, Lochsteine, Blocksteine, Hohlblocksteine (Calcium silicate blocks), 09/1980 edition
- DIN 1048, Prüfverfahren für Beton – Festbeton, gesondert hergestellte Probekörper (Testing procedures for concrete), 06/1991 edition
- DIN 4165, Gasbeton-Blocksteine und Gasbeton-Plansteine (Autoclaved aerated concrete blocks), 12/1986 edition
- DIN EN 772, Prüfverfahren für Mauersteine (Test procedures for masonry units), draft 1992
- ENV 1992, Eurocode 2 - Design of Concrete Structures, 1998

- ENV 1996, Eurocode 6 - Design of Masonry Structures, English version, draft 1996
- Hilsdorf, H.K., Reinhardt, H. W., 1997, "Beton," (Concrete) Beton-Kalender Volume 1, Berlin, Germany, Ernst & Sohn, pp. 1-150
- Kirtschig, K., D. Kasten, 1981, "Formfaktoren für die Prüfung von Mauersteinen," (Shape factors for the compressive strength of masonry units) Mauerwerk-Kalender, Berlin, Germany, Ernst & Sohn, pp. 687-703
- Marzahn, G., 2000, "Untersuchungen zum Trag- und Verformungsverhalten von vorgespanntem Trockenmauerwerk," (Investigation of load bearing and deformation capacity of dry-stacked post-tensioned masonry) PhD-Thesis, University of Leipzig, Leipzig, Germany
- Ross, A.D., 1937, "Concrete creep data," The Structural Engineer 15, No. 8
- Sell, R., 1970, "Festigkeit und Verformung von Gasbeton unter zweiachialer Druck-Zug-Beanspruchung; Untersuchung über die Gasbeton-Schubfestigkeit zum Studium des Bruchverhaltens," (Strength and deformation of autoclaved aerated concrete subjected to biaxial compression-tension) DafStb, Heft 209, Berlin, Germany, Beuth-Verlag
- Schubert, P., Friede, H., 1980, "Spaltzugfestigkeitswerte von Mauersteinen," (Tensile splitting strength of masonry units) Die Bautechnik 57, Heft 4, pp. 117-122
- Schubert, P., Gonzales, A. C., 1997, "Zugfestigkeit von Porenbeton und Haftscherfestigkeit von Dünnbettmörtel auf Porenbeton," (Tensile strength of autoclaved aerated concrete blocks and the cohesion in thin mortar layer joints) Mauerwerk-Kalender, Berlin, Germany, Ernst & Sohn, pp. 629-643